A Confocal Microscope and Raman Spectroscopy Probe for Mars exploration
by Dawn Michelle Crowder

A thesis submitted in partial fulfillment of the requirements for the degree of Masters of Science in Electrical Engineering
Montana State University

Abstract:
This thesis describes the development of a prototype Confocal Microscope and Raman Spectroscopy Probe for the application of Mars exploration. Raman spectroscopy is a useful identification tool for astrobiologists searching for biomarkers and microbial fossils as evidence of past life on the surface of Mars. Combining Raman spectroscopy with an imaging system gives morphological context to the spectral information that is necessary in order to come to an exobiological conclusion. The confocal microscope and Raman spectrometer use laser illumination at either 852 run or 1064 nm. A compact probe houses the optical systems and is linked to the laser source, spectrometer, and imaging processing electronics through optical fiber and electronic cable. The probe can be located at the end of a robot arm which facilitates in situ sample investigation during field operation. Integral to system design is the microscope's MEMS scanning system, the dispersive spectrometer (using an uncooled silicon CCD or InGaAs detector array), and the 150 mW 852 nm DBR diode laser or 120 mW 1064 nm microchip laser. This thesis presents a theoretical treatment of the confocal imaging system, probe design, optical integration with the Raman spectrometer, and experimental demonstrations. The 1064 nm probe has a field of view of 120 microns, a resolution of 1.4 microns, a spectral range from 400-4000 cm-1, measures 9 x 4.5 x 4 cm and weighs approximately 300 grams.

A CONFOCAL MICROSCOPE AND RAMAN SPECTROSCOPY PROBE FOR MARS EXPLORATION

By

Dawn Michelle Crowder

A thesis submitted in partial fulfillment
of the requirements for the degree

of

Masters of Science

in

Electrical Engineering

MONTANA STATE UNIVERSITY
Bozeman, Montana

April, 2002

APPROVAL

of a thesis submitted by

Dawn Michelle Crowder

This thesis has been read by each member of the thesis committee and has been found to be satisfactory regarding content, English usage, format, citations, bibliographic style, and consistency, and is ready for submission to the College of Graduate Studies.

David Dickensheets, Committee Chair — (Signature) — April 19, 2002 (Date)

Approved for the Department of Electrical & Computer Engineering

Jim Peterson, Department Head — (Signature) — 4/19/02 (Date)

Approved for the College of Graduate Studies

Bruce McLeod, Graduate Dean — (Signature) — 4-19-02 (Date)

STATEMENT OF PERMISSION OF USE

In presenting this thesis in partial fulfillment of the requirements for a master's degree at Montana State University, I agree that the Library shall make it available to borrowers under the rules of the Library.

If I have indicated my intention to copyright this thesis by including a copyright notice page, copying is allowable only for scholarly purposes, consistent with "fair use" as prescribed in the U.S. Copyright Law. Requests for permission for extended quotation from or reproduction of this thesis in whole or in parts may be granted only by the copyright holder.

Signature 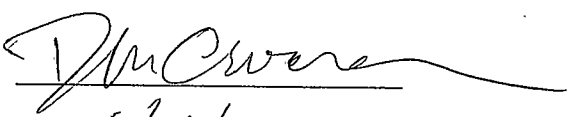

Date 4/19/02

ACKNOWLEDGMENTS

Thank you to Professor David Dickensheets, my advisor. His vision is responsible for the success of this project; and I credit his faith and optimism with my success as a graduate student. Thank you to Professor Chris Yakymyshyn for valuable advice and consultation along the way. I also appreciate the assistance of Professor Fred Cady and Professor Joe Shaw in their evaluations and in serving as members of my graduate committee.

My peers in David's group helped me tackle many obstacles. Thanks to Matt Faulhaber, Micheal Wood and Bryan Tikalsky for their direct contributions on the Image Processing portion of this project. Phil and Micheal, thank you for friendship and perspective.

I could never have completed this work without the support of my friends and family. In particular, thank you to Timme, Mel, Mary, Jacy, and Matt.

TABLE OF CONTENTS

TABLE OF CONTENTS - CONTINUED

LIST OF TABLES

Table Page

LIST OF FIGURES

Figure Page

LIST OF FIGURES - CONTINUED

Figure Page

LIST OF FIGURES - CONTINUED

Figure Page

LIST OF FIGURES - CONTINUED

Figure Page

LIST OF FIGURES - CONTINUED

Figure Page

ABSTRACT

This thesis describes the development of a prototype Confocal Microscope and Raman Spectroscopy Probe for the application of Mars exploration. Raman spectroscopy is a useful identification tool for astrobiologists searching for biomarkers and microbial fossils as evidence of past life on the surface of Mars. Combining Raman spectroscopy with an imaging system gives morphological context to the spectral information that is necessary in order to come to an exobiological conclusion. The confocal microscope and Raman spectrometer use laser illumination at either 852 nm or 1064 nm. A compact probe houses the optical systems and is linked to the laser source, spectrometer, and imaging processing electronics through optical fiber and electronic cable. The probe can be located at the end of a robot arm which facilitates *in situ* sample investigation during field operation. Integral to system design is the microscope's MEMS scanning system, the dispersive spectrometer (using an uncooled silicon CCD or InGaAs detector array), and the 150 mW 852 nm DBR diode laser or 120 mW 1064 nm microchip laser. This thesis presents a theoretical treatment of the confocal imaging system, probe design, optical integration with the Raman spectrometer, and experimental demonstrations. The 1064 nm probe has a field of view of 120 microns, a resolution of 1.4 microns, a spectral range from 400-4000 cm^{-1}, measures 9 x 4.5 x 4 cm and weighs approximately 300 grams.

CHAPTER ONE

INTRODUCTION

The study of the climate, geology, and biological history of Mars could provide a valuable link to Earth's past and future. The National Aeronautics and Space Administration (NASA) began an intensive Mars exploration program in the 1990's, aiming to find clues to the origins and history of life in our solar system [1]. In years past, the Viking landers rejected hypotheses that any life on Mars would be confined to surface habitats [2]. Instead, they exposed the surface of Mars to be a hostile environment, with an atmospheric pressure two orders of magnitude lower than that on Earth, extreme UV-radiation, little water, and a strongly oxidizing regolith [3, 4]. Twenty years after the success of Viking, the Mars Pathfinder mission confirmed this void of life at the surface of Mars, leaving future exploration efforts with two options: to search for life in localized, possibly cryptic environmental niches, or to search for the biomarkers or remains of a biological community that once existed on the surface of ancient Mars [1, 2, 3, 5].

If found anywhere, extant life on Mars would be confined to specific environmental niches removed from the harsh surface environment. Astrobiologists have postulated chemosynthetic ecosystems existing far beneath the surface in a biological "oasis" [2, 6]. However, space exploration technology presently precludes

drilling deep into Mars' crust and we are restricted to looking for evidence of present and past life within several meters of the surface [5]. An exobiological search for latent or extinct organisms involves looking "for a past atmosphere, past and present liquid water, organics and fossilized primitive systems. Analysis should be focused on carbonates, water and organics in Martian subsurface and sediments" (Brack, 1996) [7].

The presence of some form of water on the surface of present day and historical Mars suggests that though currently impossible, an environment capable of supporting prokaryotes once existed on the planet's surface [5]. Mars Global Surveyor (MGS) determined the north polar cap on Mars to be composed primarily of water ice, at a volume that is approximately one third that of the Greenland ice cap. Viking orbiters and MGS have returned thousands of surface images of the geologic remains of fluvial channels, drainage networks, and floodplains, indicating that atmospheric conditions may have once been such that liquid water flowed on the surface. In addition, it is probable that sub-surface water exists in the form of permafrost in aquifers [4, 8]. These regions are ripe areas for exobiological prospecting since much of the surface of ancient Mars is still well preserved and unweathered, and the morphological and chemical evidence of remains of organisms may still be present [2].

Cyanobacteria are a prime candidate for historical Martian surface habitation due to their remarkable tolerance of a hostile high-stress environment. On Earth, they are found in a variety of near-surface, cold desert Antarctic habitats such as on

lakebeds in living stromatolites (laminated structures built mainly by cyanobacteria), on exposed rock ridges in layered communities, and in an endolithic habitat. On Mars, similar communities may be preserved through burial and freezing. Therefore, a surface investigation searching for evidence of photosynethetic life on Mars can concentrate on cyanobacterial residues such as photosynthetic pigments, sunscreens, photoprotective minerals, and stress-protective compounds [5, 9].

Raman spectroscopy is an attractive analytical tool for detecting these organisms and their bio-markers, as it is capable of identifying both organic and inorganic substances. According to H. G. M. Edwards *et al.* it is unique in that aspect; and therefore well suited to investigate chemically the biology and the geology of its sample concurrently [10, 3]. Many types of spectrometers capable of either elemental or molecular analysis have landed on the surface of Mars to determine surface and sediment composition. Viking landers had two spectrometers included in their scientific payload: a Gas Chromatograph/Mass Spectrometer (GCMS) which performed molecular analysis and an X-Ray Fluorescence Spectrometer (XRFS), which determined elemental composition of samples [2, 4, 11]. The Mars Pathfinder sent an Alpha Proton X-ray Spectrometer (APXS) to the surface of Mars to determine the elemental chemistry of rocks [12]. Athena, which is scheduled to launch in 2003, will send a Miniature Thermal Emission Spectrometer (Mini-TES), a Mössbauer Spectrometer, and another APXS on board a pair of rovers. A non-imaging Raman spectrometer was originally included in the Athena payload but was recently moved to a subsequent mission. The Mini-TES will investigate rocks and soils around the

landing site for mineralogical information based on thermal emission spectroscopy. The Mössbauer spectrometer will investigate the oxidation state of iron, the magnetic phase in the martian soil, and iron-bearing minerals in rocks [13]. When used in conjunction with a Microscopic Imager, the elemental and molecular information obtained by the Athena spectrometers will facilitate a search for evidence of past liquid water. These spectrometers previously mentioned, as well as the spectrometers sent to orbit the planet, are gathering mineralogical, elemental, and atmospheric data which will aid in choosing an appropriate landing site for exobiological research. The next step is to send an instrument to Mars capable of identifying organic compounds (this has not been done since the GCMS, aboard Viking) [1]. Raman spectroscopy is not only suited for this task, it provides mineralogical information at the same time. Comparatively speaking, it is a rapid technique and requires no sample preparation. Raman spectroscopy need not be perceived as a replacement for other mineralogical spectroscopy techniques; rather, it is enhanced by the information provided in both elemental and other molecular techniques [14].

Raman Spectroscopy

Raman scattering was discovered in 1928 by two Indian scientists, Raman and Krishnan [15]. When light is scattered by a molecule, a shift in frequency may be observed due to an inelastic interaction with the vibrational modes of the molecule. The frequency shift can be positive or negative, depending on the initial energy state of the molecule. Scattered light that loses energy to the vibrational modes of the atom

is called Stokes Raman-shifted light, whereas scattered light that increases in is called anti-Stokes Raman-shifted light. The Stokes spectrum is much stronger than the anti-Stokes since Stokes scattering involves molecules that are initially in a ground energy state. Because anti-Stokes scattering occurs when light is incident upon molecules already in an excited vibrational energy state (which has a low probability of occurrence) the anti-Stokes spectrum is much weaker. However, both the Stokes and anti-Stokes scatter are dwarfed by Rayleigh scattering, which dominates by at least three orders of magnitude [16, 17, 10].

Raman spectroscopy is a method that uses Raman scattering to identify different materials. A narrow linewidth source illuminates a sample, and the scattered light is collected. Rayleigh scattered light is filtered out and the Raman peaks are recorded as a function of relative energy. The resulting spectrum can be used as a fingerprint to identify materials via their different vibrational energy modes. The vibrational energies of molecules and crystals lie in between zero and 5,000 wavenumbers. A wavenumber represents the number of wavelengths per centimeter and is written as cm^{-1} [16]. A Raman spectrum plots emission intensity versus frequency shift relative to the frequency of the source illumination [18].

Conventional Raman spectrometers use high power lasers in the visible region to near-infra-red region(NIR) and require sensitive, cooled detectors. As a result, most Raman systems are large table-top instruments. Recent technology advances in narrow linewidth high power diode lasers and sensitive CCD arrays have reduced the bulk of spectroscopy equipment considerably. The reduction in size, weight and

power consumption has made them available for *in situ* field use by consumers, and now for spaceflight and planetary exploration.

Wang *et al.* at Washington University in St. Louis have developed a breadboard instrument for a Raman spectroscopic sensor designed for *in situ* planetary surface investigations. Similar to commercial Raman field instruments, a probe illuminates the sample and collects a light signal remotely from the spectrometer and power supply, through optical fiber and electronic cable (see figure 1.1). The visible diode laser source is located in the probe head and illuminates a spot

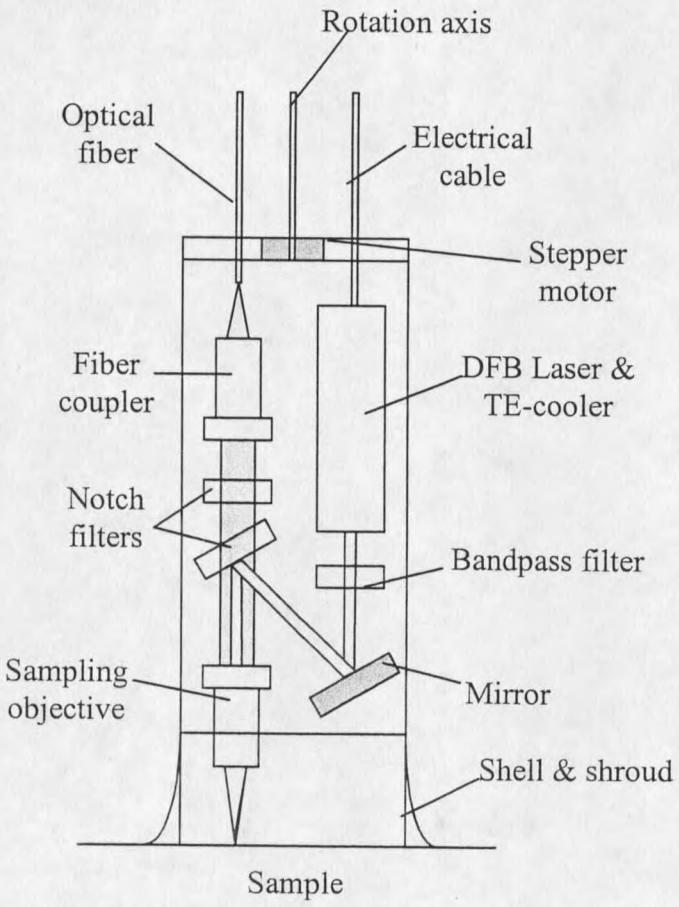

Figure 1.1 Cross-section diagram of Raman probe built by Wang *et al.*

size of about 20 microns on the sample. Once the probe is placed on the sample by a robotic arm, the instrumentation inside rotates with respect to the shroud. The objective lens is located off-axis, which enables a scan of the sample and results in a curved line scan of the rock's mineralogy. Spectra are taken from each point (approximately 20 microns in diameter) along this curvilinear line [14].

Wdowiak *et al.* at University of Alabama Birmingham also discuss a laser Raman spectrometer system for lander spacecraft, but details of their design are not known at this time [19].

Combining Raman Spectroscopy with Confocal Microscopy

Molecular information must be coupled with morphologic evidence and climate information to come to an exobiological conclusion. The Athena payload includes the Microscopic Imager to give context to the spectroscopic data and to look for morphological information [20]. Combining an imaging system with a spectrometer would not only provide two legs of the tripartheid proof needed in exobiology, it could allow for composition to be linked directly with morphology on a microscopic scale.

Our unique instrument designed for Mars surface investigation combines a Raman spectrometer with a confocal laser scanning microscope (CLSM) capable of *in-situ* operation. The CLSM is chosen as the imaging companion to the Raman system because of the compatibility of these two systems. The only fundamental change the confocal microscope makes in the optics of a Raman collection probe is

the scan mirror, which scans the beam to construct an image. The CLSM miniaturizes well (compared to CCD imaging systems) and offers superb resolution with simple optics. The Confocal Microscope and Raman Spectrometer (CMaRS)

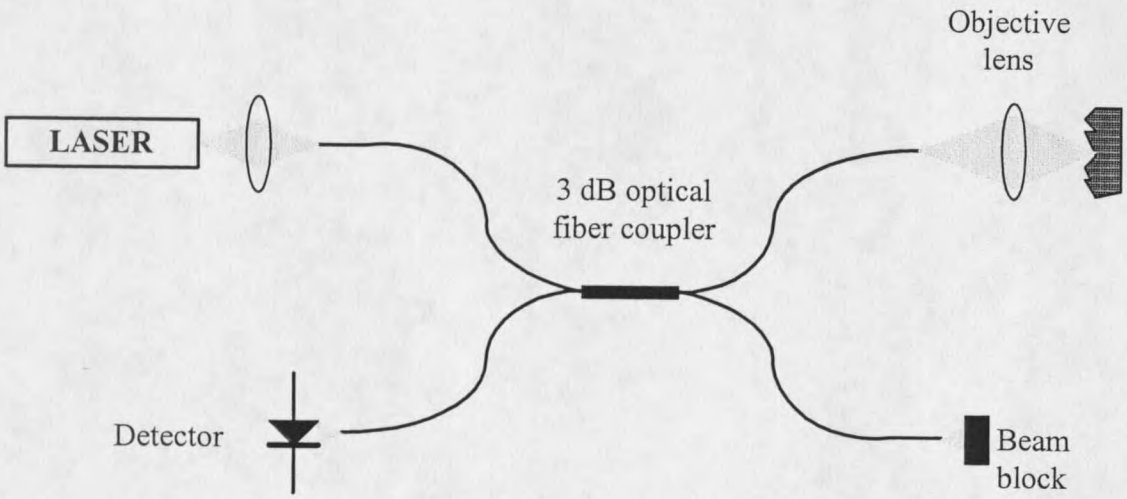

Figure 1.2 Schematic of a fiber confocal optical microscope. Note that the objective lens (and any other necessary light collection optics) are separated from the light source and the detector by some arbitrary length of optical fiber.

can acquire a reflection-based image of a sample and then take Raman spectra from various locations within the field of view of 300 microns.

The confocal optical microscope differentiates itself from the conventional white light microscope by its shallow depth of focus. This makes it a useful instrument for cross sectional imaging and sample profilometry as well as accurate height and thickness measurements [21]. A pinhole is placed at the illumination and detection points of the microscope which eliminates the collection of any rays that are not scattered from the front focal plane of the objective lens. Thus when an object is

out of focus, it does not appear at all, whereas with a conventional microscope it would appear blurry. In 1988, Harris invented the fiber-optical scanning confocal optical microscope, in which optical fiber acts as both the source and detector pinhole [22]. This simplification of the optical design not only miniaturizes the microscope as a whole, but also allows the source and detector to be separated from the light collection optics through an optical fiber, as shown in figure 1.2. Consequently, the microscope can be used for *in situ* investigations, with the source, detector and electronics located remotely from the lens. A confocal optical microscope can image only one point at a time. Consequently, either the sample, the illumination beam, or the objective lens must be scanned in order to obtain an image with an acceptable field of view. However, both sample scanning and objective lens scanning are bulky and slow, and not suited for *in situ* imaging. Most commercial confocal scanning optical microscopes use beam scanning to create an image. Beam scanning can be achieved by either scanning the pinhole or using a galvanometer mirror [21].

The CMaRS integrates the optical systems of a confocal scanning optical microscope in with a Raman spectrometer, creating an *in* situ investigation tool for exobiological and mineralogical studies. The microscope and spectrometer share the same source illumination and light collection optics, which keeps size and weight to a minimum. A Micro-Electro-Mechanical Systems (MEMS) two dimensional torsion scan mirror rasters the beam across the sample and the reflected light generates a real time image. Raman spectra can be taken over the entire field of view, a reduced field of view, or from a focused spot within the field of view. Unlike other prototype

Raman spectroscopy instruments proposed for space exploration, the CMaRS combines microscopic imaging with Raman spectroscopy to create a powerful diagnostic tool in both biological and geology investigations.

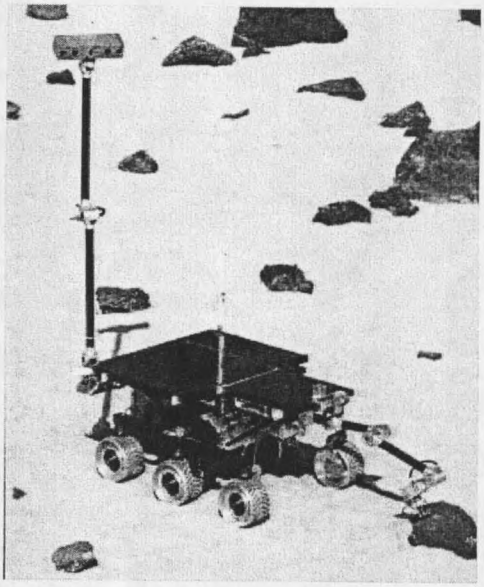

Figure 1.3 NASA photograph of FIDO. A similar rover will house the CMaRS system with the probe located on the end of the robot arm.

The CMaRS is intended for a robotics exploration of Mars and thus designed for rover-based operation. To achieve this, the bulk of the instrument must reside on the rover body, itself. A compact and lightweight probe contains only the necessary elements for sample illumination and light collection. Optical fiber and electronic cabling will route signals from the probe to the rover body where image processing and spectral analysis take place.

Thesis organization

This thesis will discuss the development of the CMaRS to the brassboard

stage. Chapter two provides a general overview of the entire CMaRS system. The remaining chapters focus on my contributions to this project which include: the CMaRS probe design, operation, and interfacing with the other sub-systems. Chapter three discusses the design of the confocal scanning microscope within the probe, with some theoretical analysis included. The Raman spectroscopy portion of the probe design is addressed in Chapter four. Chapter five includes the specifications for the probe as well as images and spectra taken by the CMaRS. Finally, I will conclude this thesis in Chapter six, discussing the successes and shortcomings of the CMaRS instrument and outlining future instrument development.

CHAPTER TWO

INSTRUMENT OVERVIEW

The CMaRS instrument can be divided into four sub-systems: light launch, probe, image processing and probe control electronics, and spectroscopy system. These sub-systems and their over all integration into the CMaRS instrument are designed for remote field applications. All components except the probe will reside in a compact and environmentally shielded box that sits on a rover body in the case of remote operation or in an operating station. The probe can be deployed to the precise sample location for information collection. Communication from the probe to the

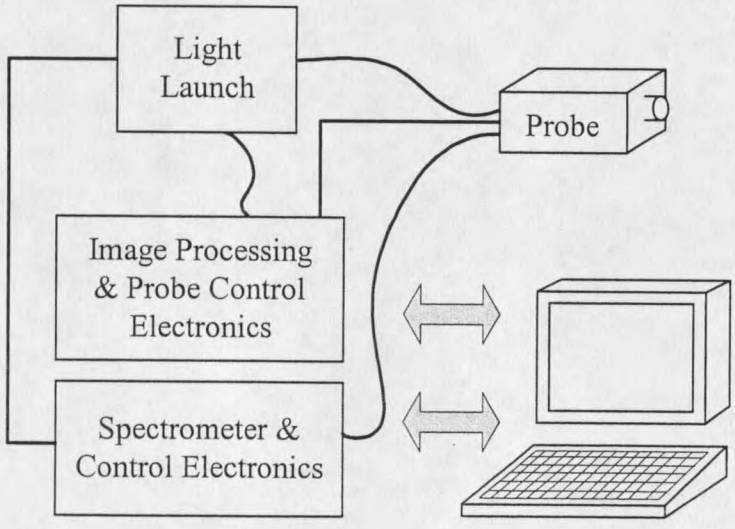

Figure 2.1 Block diagram for the CMaRS instrument. Electrical connections are denoted by straight lines, optical connections are shown as curved lines.

CMaRS instrument body is done through optical fiber and electronic cable. Software on a personal computer provides a user interface and displays spectra and images. Figure 2.1 illustrates the links between these systems that make up the CMaRS instrument.

To date, two versions of the CMaRS have been created at two different wavelengths of light. Consequently, each version is unique in its light launch and spectrometer systems. The probe and the image processing and control electronics are nearly identical for both instruments, however. The CMaRS system was originally developed at 852 nm and this thesis will refer this instrument as the CMaRS 852 when the distinction is necessary. The second system constructed uses a 1064 nm laser and will be referred to as CMaRS 1064. Most of the imaging analysis will be treated at 1064 nm, whereas the spectroscopy system will discuss the CMaRS 852.

Light Launch

The light launch portion of the CMaRS system encompasses the delivery of illumination light to the probe as well as the returned confocal signal to the photodetector and electronics board. Figure 2.2, is a modification of figure 1.2, where the 3 dB fiber coupler commonly used in a fiber confocal optical microscope has been replaced with a free space beam splitter. The area within the dotted lines is the 'light launch' system and will be discussed briefly in this section.

The light source for the CMaRS 852 is an 852 nm distributed bragg reflector (DBR) diode laser. The narrow linewidth and high power of this laser are essential to the resolution and sensitivity of the spectrometer. The laser light is collimated, travels through a polarizing beam splitter, and is then focused into a polarization maintaining (PM) single mode (SM) optical fiber. This fiber supplies the remotely located probe with illumination light as well as collects the confocal signal. The returning light is cross-polarized to the outgoing light, so when it reaches the polarization beam splitter, it is reflected instead of transmitted. As is shown in figure 2.1, this reflected light is routed through a multi-mode (MM) fiber to the photodetector. At this point, the confocal signal enters the image processing system. The light launch for the CMaRS 852 is not ruggedized or field-ready. Light launch for the CMaRS 1064, however, was constructed and packaged for field use. The 1064 laser is a diode pumped NdYAG microchip laser coupled directly to the beamsplitter assembly shown in figure 2.2. Replacing the lenses with GRIN (Gradient Index) rods, it essentially uses free space elements that are cemented together and butt-coupled into the optical fiber. The laser system was built by C.P. Yakymyshyn for TRI, Inc.

Polarization optics are used in this module for two reasons. One is to conserve light and avoid loosing 50% of the illumination each way with a regular beam splitter. The second reason is to isolate the laser source from the scattered light. Any feedback into the laser could cause instability in its intensity output.

CMaRS Probe

The CMaRS probe serves two functions: it delivers light to the sample and then collects the backscattered signal, filtering the Raman signal from the imaging signal and sending each to their respective detectors through optical fiber. Figure 2.3, is a conceptual drawing of the basic elements in the probe.

Light entering the probe is immediately collimated and passes through some Raman filters unimpeded. A quarter wave plate (QWP) circularizes the previously linearly polarized light so that upon reflection, the returning confocal signal will have

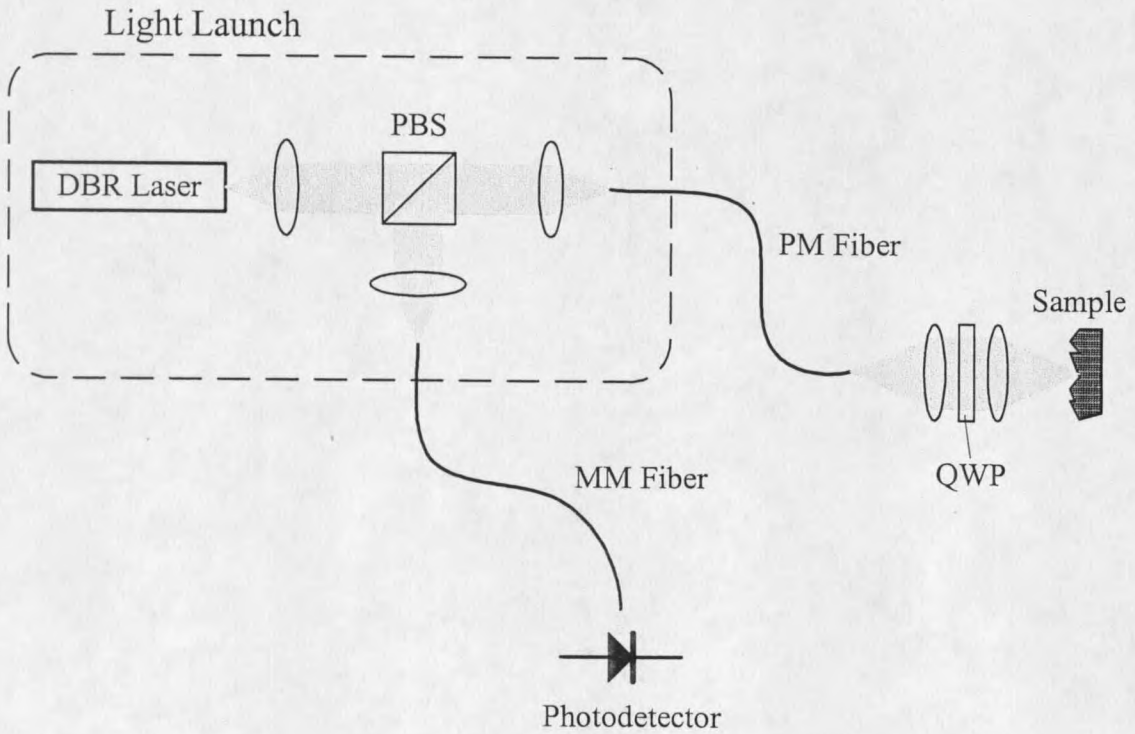

Figure 2.2 A fiber confocal optical microscope with a free standing polarizing beam splitter (PBS) instead of a fiber coupler. This is the configuration of the confocal imaging portion of the CMaRS instrument. 'QWP' is an abbreviation for 'quarter wave plate.'

an opposite polarization orientation compared to the incoming illumination. Then, a folding mirror directs the beam onto the MEMS scan mirror that rasters the beam in two dimensions, determining the field of view for the microscope. A lens relay

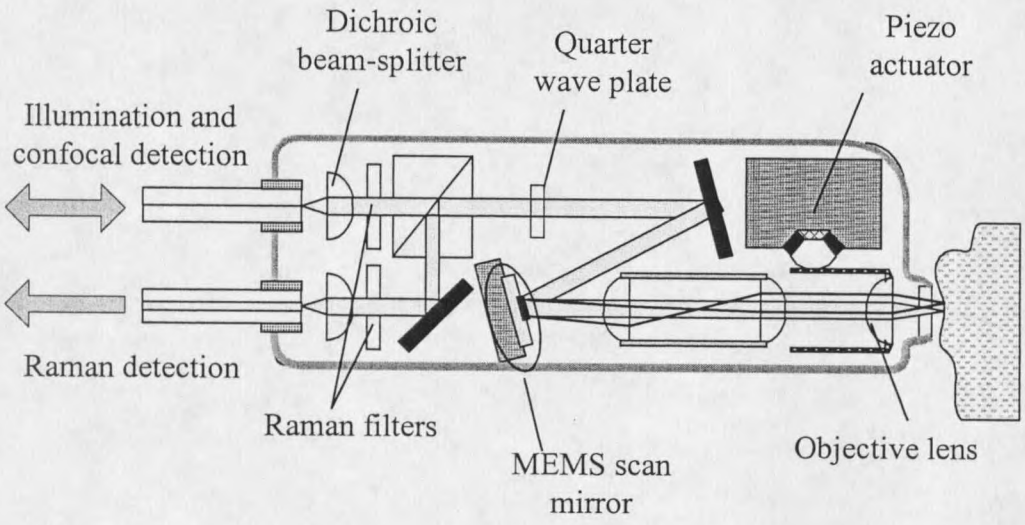

Figure 2.3 Conceptual drawing of CMaRS probe.

magnifies the beam by a factor of 2.3 and images the scan mirror in the back focal plane of the objective lens. The objective lens focuses the illumination light onto the sample. Light that is backscattered off of the sample is collected by the objective lens and retraces the optical path towards the collection fibers. This scattered light contains both spectral and image information from the sample. The elastically scattered light constitutes the imaging signal and is coupled directly into the same single mode fiber from which it originated. A dichroic beamsplitter in the beampath separates the spectral information from the imaging signal by passing the elastically scattered light and reflecting the Stokes Raman shifted light. The Raman shifted light

is then routed through a long pass filter before it is coupled into a multi-mode fiber and delivered to the spectrometer.

The MEMS scan mirror (a product of Microvision, Inc., in Bothell, WA) is an essential element for the CMaRS probe, without which this level of miniaturization would not be feasible. It is not only compact and robust, but it outperforms its larger alternatives, scanning in two dimensions fast enough for real time imaging. The two dimensional imaging capabilities of the CMaRS probe are enhanced by a focusing mechanism that provides the third dimension. Figure 2.3 shows a piezo-actuator located in the upper right hand corner of the CMaRS layout. This actuator drives the objective lens forward and backward to allow for one millimeter of focus control. The probe can be pressed up against a sample and the objective lens is moved to find the optimum focus. Together with video-rate two-dimensional imaging, the focus control allows the user to perform image profilometry on a sample. Since confocal microscopes only image one plane at a time, by physically stepping through image planes in discrete increments, CMaRS can investigate the surface relief of a sample. Post processing of the profile images is an option that allows the user to construct a composite image combining the features of each layer into one extended depth-of-field image.

Image Processing and Probe Control Electronics

The hardware and software for the probe are responsible for data signal acquisition, video signal generation, scan mirror control and focus control. This is

accomplished through four separate electronics modules: the Scan Converter (SC), the Microvision Electronics Module (MEM) and the Micropulse Systems Electronics Module (MSEM), and controlled by the user through the Software Control Interface (SCI). The MEM and MSEM receive conditioned power from and are controlled by the SC.

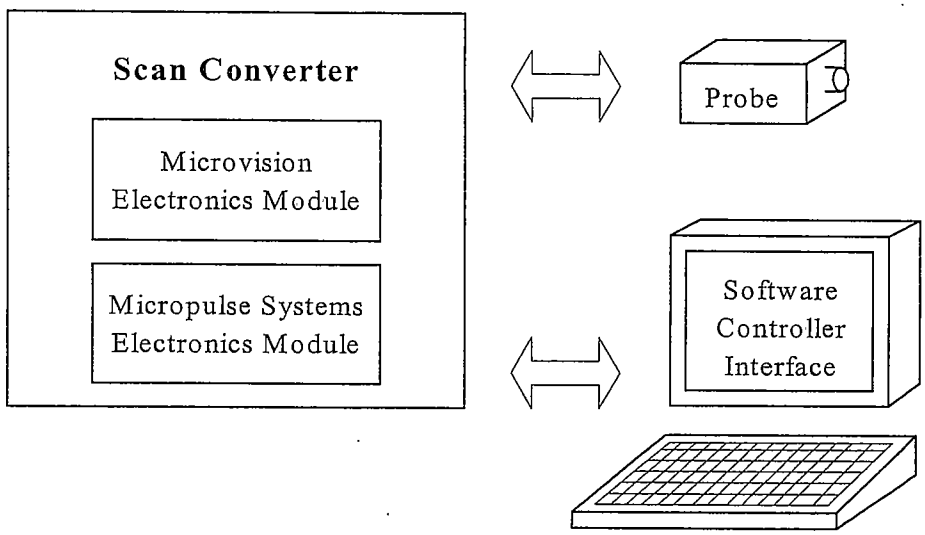

Figure 2.4 Image processing and probe control electronics block diagram

The SC receives the optical image signal and amplifies it, converts it into digital image frames, and then converts these frames into a continuous data stream in an NTSC video signal format. Through the SCI, the user can choose to watch free-running video or individual video frames on a computer monitor. Scan Mirror control is shared between the SC and the MEM. The MEM drives the horizontal axis of the mirror at its natural frequency and provides a horizontal synchronization signal to the SC. The SC uses this horizontal sync signal to generate the vertical scan signal and a frame. The user can power these on and off and adjust the scan amplitude of the

vertical axis through the SCI. The MSEM activates the dynamic focusing system on the probe. Focus control is interfaced from the user to the MSEM through the SCI and the SC. Development and coordination of these systems was done by M. J. Faulhaber, M. T. Wood, and B. Tikalsky.

Spectroscopy System

The Raman Spectroscopy System for the CMaRS is developed and built by Top Raman Instruments (TRI) of Laramie, Wyoming. TRI works together with Micron Optical to produce a line of compact, field rugged spectroscopy instruments.

Spectrometer development and availability has governed the CMaRS source illumination choice. TRI manufactures Raman Spectrometers at 633 and 852 nm for commercial use, and a 1064 nm system is currently under development. The CMaRS prototype instrument has been built at both 852 nm and at 1064 nm, thus using the Solution 852, which is TRI's 852 nm spectrometer, and their development version for 1064 nm. Each spectrometer has its own design, some of which is dictated by wavelength dependent components such as the detector. However, the design concept is comparable for both, based on a Czerny-Turner dispersive spectrometer design.

The Raman filters housed in the CMaRS probe separate the Raman back-scattered light from the confocal signal. This light is delivered to the spectrometer through a multi-mode optical fiber. As Raman scattering is a weak process, it is important to maximize the light collection capabilities of the probe and use a fiber

with a well-matched numerical aperture and a large core size. However, due to spectrometer design in this case, fiber core size effectively dictates spectrometer resolution and a balance is reached using a 50 um core step index fiber for Raman light collection.

The TRI spectrometer design is based on the Czerny-Turner spectrograph (see figure 2.5). Light entering the spectrometer is directed onto a grating. Diffracted light is spread according to wavelength and routed to a detector. The grating is stationary so a position sensitive array must be used as a detector. The 852 system uses a silicon CCD (charge coupled device) camera whereas the 1064 system uses an InGaAs camera. Figure 2.5 shows a zig-zag design which incorporates curved mirrors. The TRI design is a variation of this, using on-axis optics to eliminate astigmatism that would create measurement error with a pixel-based position-sensitive detector.

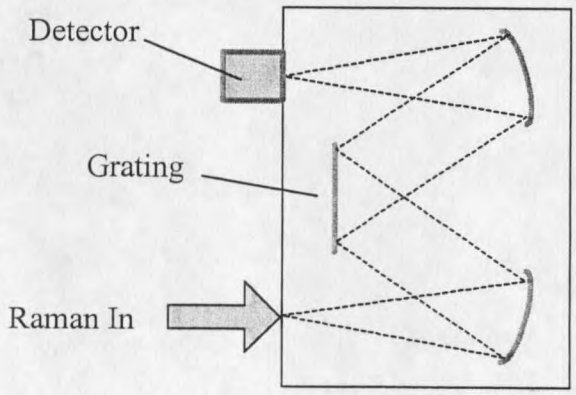

Figure 2.5 The Czerny-Turner spectrograph.

This thesis will not address spectrometer design in any further detail. Instead, the following chapters will concentrate on how the spectrometer interfaces with the CMaRS system as a whole, and specifically, with the CMaRS probe. Results in chapter 5 will include examples of spectra taken by the Solution 852 using the CMaRS probe as the light collection device.

CHAPTER THREE

CONFOCAL DESIGN

The basic elements required to build a confocal scanning optical microscope (CSOM) are point illumination, point detection, a confocal lens system, and a method of scanning the sample [21]. In the introduction, the basic elements of the CMaRS were discussed briefly. An optical fiber provides the point illumination and point detection for the microscope. A MEMS scan mirror is used to scan the beam across the sample, instead of moving the sample itself. This chapter will address these elements in further detail and introduce the optical system, as well as the general layout and design of the probe. Theoretical performance measures and system simulations will also be presented.

Optical Design

Design constraints

The confocal imaging system is designed to interface with the Raman spectrometer. A several hundred micron field of view would encompass a large enough sample region to determine morphological information. Design goals for the CMaRS are a field of view of 300 microns and a spatial resolution of 1 micron. These design parameters are primarily dependent upon the scanning angle of the scan mirror, and the effective numerical aperture (NA) and focal length of the objective lens.

The image for a confocal microscope is built up point by point using a scanning mechanism; and in the case of the CMaRS, this is accomplished by rastering the beam across the sample with a scanning mirror. The placement of the scanning mirror is critical to the performance of the microscope. To ensure a constant magnification regardless of the focus position, the system is telecentric, meaning the entrance or exit pupil must be located at infinity [23]. Placing the scanning mirror in the back focal plane of the objective lens prevents vignetting of the reflected beam and keeps the image created by the microscope from becoming distorted. (See figure 3.1)

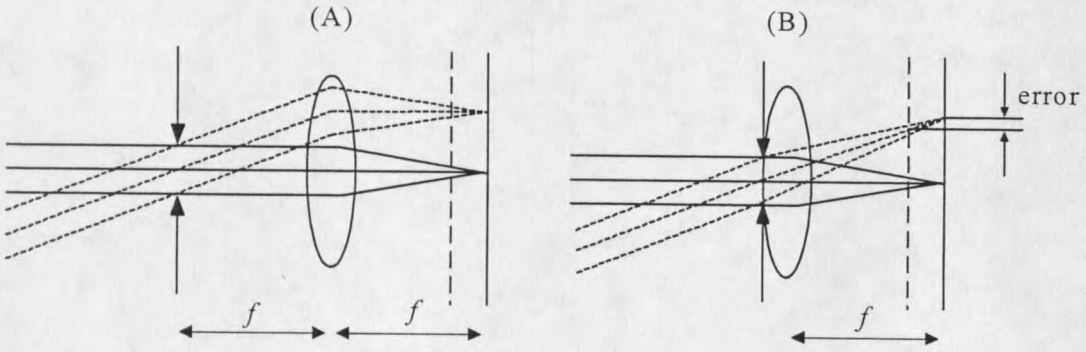

Figure 3.1 This figure illustrates the telecentric stop and its importance for beam scanning systems. If the scanning element is placed in the back focal plane of the objective lens, or at the telecentric stop, as it is in diagram A, the image is accurate whether the object is in the focal plane or slightly out of focus (depicted by the dotted line). Diagram B illustrates a scanning element that is not placed at the telecentric stop. Note the error in image size when the object is slightly out of focus versus when it is in focus [23].

Optical Path

The optical design strives to accommodate these constraints. Light entering the probe from the fiber is collimated and travels a zig-zag path towards the sample.

From the fiber end-face to the folding mirror it travels approximately 4.3 cm, passing through Raman filters and a quarter wave retarder. The folding mirror reflects this light at a 45 angle onto the MEMS scan mirror, 1.5 cm away. The scan mirror re-directs the beam parallel to its original path toward the sample. It travels approximately 6.35 cm through a beam expander, the objective lens and a sapphire window before it hits the sample. Light reflected off of the object re-traces its path back to the optical fiber.

The excitation beam and the reflected signal beam are limited in area by the scan mirror, which acts as the aperture stop for the system. This aperture dictates the

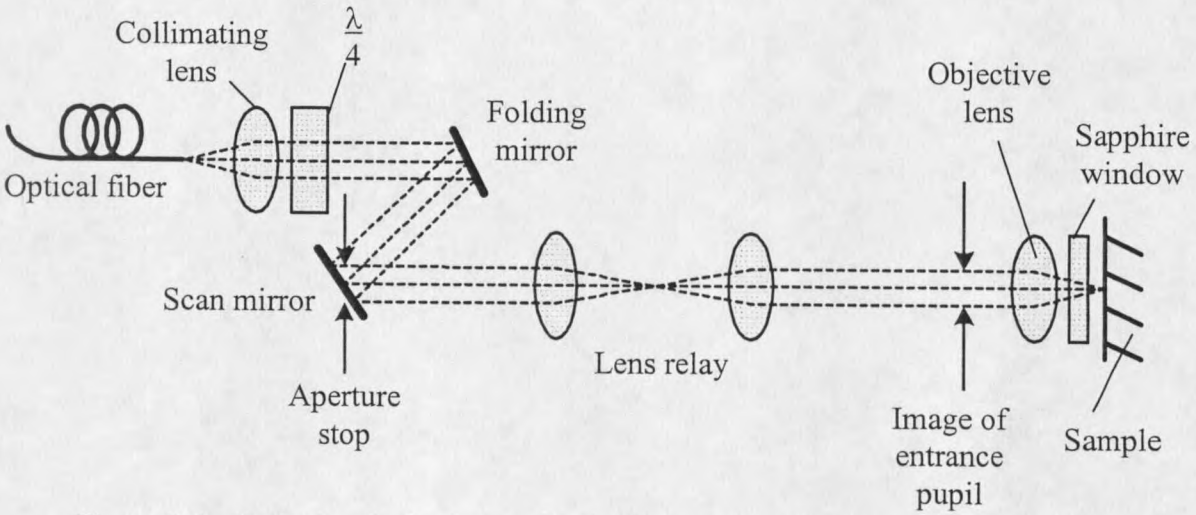

Figure 3.2 Optical path for the confocal microscope. (This diagram does not include any interface optics for the Raman spectrometer.)

size of the collimated beam entering the system via the optical fiber and collimating lens. The aperture stop for the system is imaged in the back focal plane of the objective lens, resulting in a telecentric system. The exit and entrance pupils are located at infinity.

The following sections will discuss the necessity of each of these elements as well as their specifications and any tolerances involved with their precise location in the optical path (with the exception of the Raman filters, which will be discussed in detail in chapter 4).

Lens choices

Though it is desirable to place the scanning mechanism in the back focal plane of the objective lens, due to the geometry of the MEMS scan mirror and its magnetic enclosure and mount, it is physically impossible to do so. To accommodate this, a lens relay images the scan mirror into the back focal plane of the objective lens, concurrently expanding the beam. This beam expansion is desirable to increase the effective numerical aperture of the microscope. The beam is collimated to measure approximately one millimeter in diameter at the $1/e^2$ intensity point. In using a 2.3x beam expander, the beam will be roughly 2.3 millimeters in diameter when it reaches the objective lens.

All lenses used in the CMaRS probe are molded aspheric lenses manufactured by Geltech, Inc. The glass material is a Corning derived C0550 and the difference in index of refraction between the lens design wavelength of 780 nm and the operating wavelength of 852 nm is negligible (0.0018). The lenses are coated with a multi-layer broadband anti-reflection coating that provides less than one percent reflection between 650 and 1050 nm.

The lens relay is made up of Geltech lenses 350240 and 350280. These lenses have effective focal lengths of 8 mm and 18.4 mm, respectively. This creates a beam expansion of 2.3x, and a scan angle reduction of the same magnitude. Figure 3.3 illustrates the placement of the lenses with respect to the scan mirror. The design

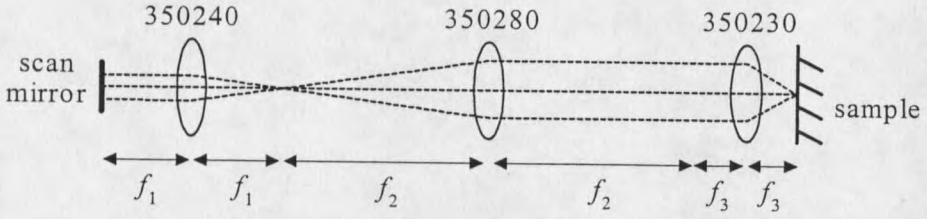

Figure 3.3 Layout for the lens relay and objective lens. In the diagram, f_1 is equal to 8 mm, f_2 is equal to 18.4 mm, and f_3 is the focal length for the objective lens (4.5 mm).

images the scan mirror in the back focal plane of the objective lens, creating a telecentric system that will produce accurate images consistently throughout the scan range.

The objective lens, Geltech part number 350230, has an effective focal length of 4.51 mm and a NA of 0.55. An incident beam measuring approximately 2.3 mm (at the $1/e^2$ intensity point) reduces the effective NA to 0.25. This focal length provides a compromise between the desired field of view and resolution of the microscope. With this focal length and beam diameter, the theoretical diffraction limited spot waist, ω, is 1.36 microns ($\omega=\lambda/\pi\theta$, where θ is the angle of the $1/e$ ray relative to the optical axis in the sample space). The field of view is then dependent upon the scan angle of the scan mirror. An optical scan angle of 6°, zero to peak and measured at the scan mirror (which is well within the specifications of the mirror)

translates roughly to a field of view of 475 microns which would meet the design goals for the CMaRS.

Polarization

The CMaRS light launch and probe systems employ polarization controlling optics for two reasons. One is to avoid interference effects in the confocal image due to the long coherence length of the laser. The second reason is to ensure maximum possible light efficiency for both imaging and Raman spectroscopy.

Light leaving the laser diode is linearly polarized, aligned with the short axis of the elliptical beam. It is incident upon a polarizing beam splitter, oriented such that most of the light is coupled into a polarization maintaining (PM) optical fiber and delivered to the probe. As was discussed in the 'Light Launch' section of chapter two, the imaging signal that returns through this same fiber will have an orthogonal polarization to the excitation light, thus it will reflect from the polarizing beam splitter instead of passing through and being coupled back into the laser. For the CMaRS 852 prototype instrument, the light launch is a free-space system, and uses a cube beam splitter and conventional bench-top optics. A half wave retarder simplifies launching the linear polarized light into the primary fiber axis. This is a bulky solution with little tolerance for changing temperatures and impractical for field use. As was mentioned in Chapter two, the CMaRS 1064 source environmentally packages the same launch system used for the CMaRS 852. The half wave retarder is not necessary for this system, as once coupling is optimized, the optics are cemented together. Other possible solutions for environmentally rugged light launch

modifications include using a polarization maintaining 3-dB fiber coupler or fiber coupled optical circulator.

The PM fiber is connectorized such that light enters the probe polarized in a horizontal direction. For the purpose of this thesis, this axis will be referred to as the x-axis, and we can call this TM polarization. TM polarized light is preferred (over TE) because the transmission curve through the dichroic filter versus angle of incidence is consistently higher than that of the TE light. The transmission is also more constant over a larger span of incidence angle for TM than for TE, which is important since precise angular alignment of this filter is not guaranteed. This will be discussed further in chapter 4, where the Raman filters are examined in detail.

Inside the probe, a quarter wave plate in the beam-path circularizes the polarization of the beam. With each reflection along the optical path, the polarization changes handedness. The beam reflects off of the folding mirror, the scan mirror, and finally off of the sample before returning to the quarter wave plate (via another reflection off of the scan mirror and the folding mirror). Thus when the beam passes through the quarter wave plate a second time, it has opposite handedness with respect to when it came out of the quarter wave plate. The quarter wave plate converts it back to linearly polarized light, but now it is of the opposite orientation from the incoming light. Thus the excitation light that is delivered to the probe through the PM fiber is horizontally linearly polarized, whereas the elastically scattered confocal signal that enters the fiber is vertically polarized. When the confocal signal light has traveled through the fiber and is incident upon the polarizing beam splitter within the

light launch system, it will be transmitted instead of reflected, as it is cross polarized opposite to the laser light.

In practice, tracking the polarization of the beam is a bit more complex, as the quarter wave plate is not the only optical element modifying the polarization of the beam. A window in the probe housing is necessary for environmental protection of the instrument. Sapphire is our the material of choice with its hardness properties and scratch resistance, however its birefringence adds to the retardance of the quarter wave plate and complicates alignment.

Imaging Capabilities

A simplified confocal microscope model is useful for a theoretical performance analysis. A complete mathematical treatment will not be discussed in this thesis. The reader can refer to Dickensheets [24], Gu, Sheppard and Gan [25] and Wilson and Sheppard [26] for an involved study of image formation for the confocal microscope. For the simplified diffraction limited confocal microscope it can be shown that:

$$I = \left| p^2 * s \right|^2 \qquad (3.1)$$

where $s=s(x,y)$ is the sample reflectivity and $p=p(x,y)=p(r)$ is the field of the optical beam in the sample plane (let $r^2=x^2 + y^2$). If we assume the sample to be a perfect point reflector, then $s(x,y)$ becomes a delta function and $I=|p(r)|^4$. This is the intensity point spread function (PSF) of the simple fiber confocal optical microscope

FCOM as shown in figure 3.4. Considering a gaussian beam input to this system, the PSF becomes [25]:

$$I(r) = \left| \sqrt{I_0} \frac{2\pi a_0^{\,2} \omega_0}{\lambda f \omega} \int_0^1 e^{-(a_0 \rho / \omega)^2} J_0(2\pi a_0 r \rho / \lambda f) \rho d\rho \right|^4 \qquad (3.2)$$

This is essentially the Hankel transform of a Gaussian field distribution at the pupil [24]. In this equation, a_0 is the radius of the pupil at the objective lens, ω is the Gaussian beam field $1/e$ radius at the objective lens, ω_0 is the mode field radius of the beam measured at the fiber endface, f is the focal length of the objective lens, and ρ is a unitless aperture variable (ρ=1 at the edge of the aperture). I_0 is the on-axis intensity at the fiber end-face and the quantity $I_0 \omega_0/\omega$ is the peak field strength at the pupil center where the beam has expanded to a width, ω. The field at the pupil can be found from the field at the fiber end-face, indicated in figure 3.4.

A parameter

Gu, Sheppard, and Gan of the University of Sydney in Australia introduced a dimensionless parameter, the 'A-parameter' which simplifies a transfer function

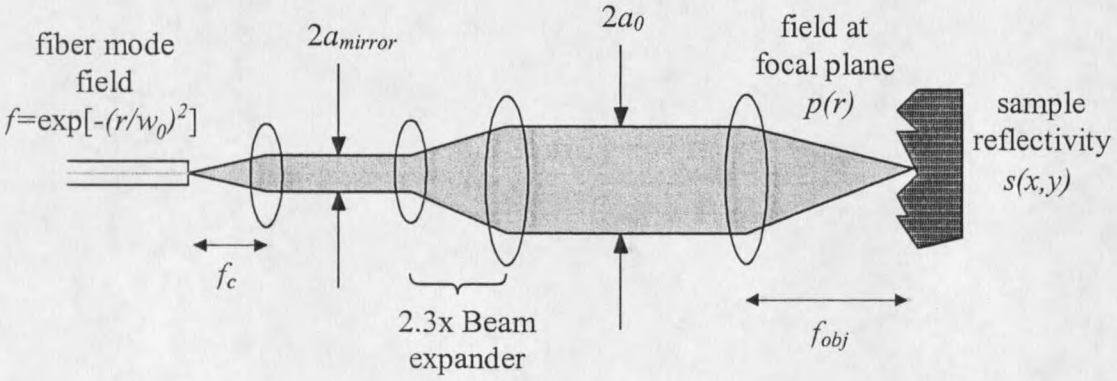

Figure 3.4 The simplified fiber confocal optical microscope. The pupil is between the two lenses, indicated by the arrows, with radius a_0.

analysis of a fiber confocal microscope. [25] They define 'A' as:

$$A = (2\pi a_{mirror} r_0 / \lambda f_c)^2 = 2(a_0 / \omega)^2 \qquad (3.3)$$

where r_0 is the intensity $1/e$ radius ($r_0=\omega_0/\sqrt{2}$) and f_c is the focal length of the collimating lens and a_{mirror} is the aperture radius at the scan mirror . The A-parameter can be conceptually considered as a dimensionless parameter proportional to the square of the ratio of the pupil radius to the Gaussian beam $1/e$ field radius. Theoretical analysis of a fiber confocal microscope's performance in terms of the A parameter is convenient for design. This section will address the point spread function, the axial response and the efficiency of the microscope with respect to A via a numerical analysis using MATLAB.

For the CMaRS probe, the aperture stop is at the scan mirror. Though the mirror is square, the rest of the system exhibits circular symmetry and in order to simplify calculations, the mirror is often considered as a circular aperture within the scope of this thesis. The length of one side of the square mirror (1.4 mm) is taken as the diameter of the pupil (as opposed to using the diagonal of the square.) The physical aperture stop (radius a_{mirror}) is imaged into the back focal plane of the objective lens by the beam expander, and this image can be considered the effective aperture for our system, a_0, and is used for image analysis. See figure 3.4 for a graphical representation of this. For the CMaRS probe, a_{mirror}=0.7 mm, and $a_0=(2.3)a_{mirror}$, where 2.3 is the magnification of the beam expander. These aperture dimensions are fixed, therefore, control over the A parameter resides in varying the size of the

incoming collimated beam. The beam waist at the pupil behind the objective lens is found to be $\omega=2.3(\lambda f_c)/(\pi\omega_0)$, where f_c is the focal length of the collimating lens and

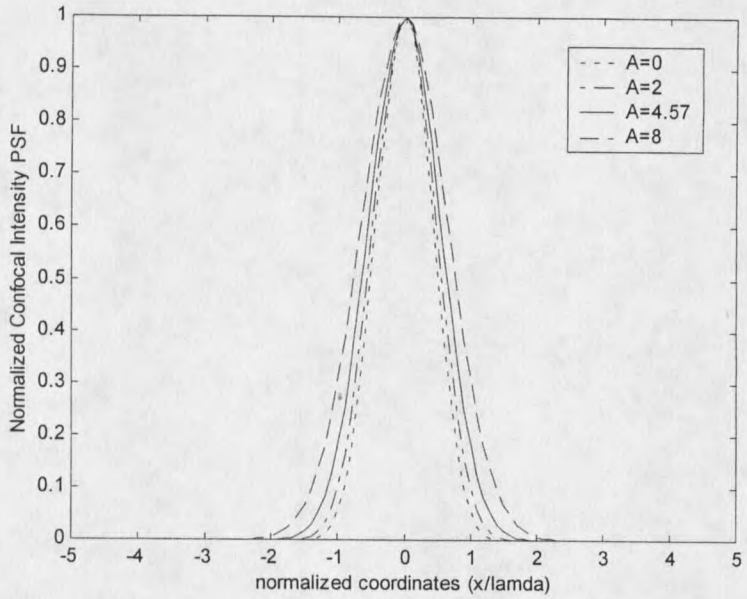

Figure 3.5 Normalized confocal point spread function for different values of A, NA = 0.25. The solid line indicates the actual curve for the CMaRS when A=4.57.

ω_0 microns is the mode field radius leaving the fiber. For our microscope, f_c=4.51 mm and ω_0=3.3 microns.

Considering these two apertures, a_{mirror} and a_0, and their respective beam waists, the A parameter and the numerical aperture can be calculated for the CMaRS. For λ=1064 nm, A=4.57 and when λ=852 nm, A=4.6. The numerical aperture (NA) for the CMaRS can be approximated as NA= a_0/f_{obj}=0.335. The beam waist does not

fill this aperture, however, so the effective numerical aperture is found to be $NA_{eff}=\omega/f_{obj}=0.25$.

Point Spread Function

The confocal point spread function (PSF) is a measure of the resolution of the microscope. Substituting the A-parameter into equation 3.2 causes the intensity PSF to be [25]:

$$I(r) \propto \left| \int_0^1 e^{-\frac{A}{2}\rho^2} J_0(2\pi \frac{a_0}{f\lambda} r\rho)\rho d\rho \right|^4 \qquad (3.4)$$

Figure 3.5 shows the theoretical intensity PSF ($|p(r)|^4$) plotted versus the focal plane radial coordinates normalized to λ. Each curve corresponds to a different value of A. Note that for the case where A=0, the first minimum point is at 1.8 microns at λ=1064 nm. An A parameter equal to zero corresponds to an infinitely wide beam waist, or a 'top-hat' illumination. The Fraunhofer diffraction pattern for a uniformly illuminated circular aperture is an Airy pattern. This pattern predicts the first minima (or zero point) in the intensity distribution to be located a distance, r=(0.61)λ/NA. In this case, for λ=1064 microns and NA=0.335, r=1.9 microns. We must remember that the Fraunhofer diffraction pattern is a paraxial approximation. With a fully illuminated pupil, the NA for the CMaRS is 0.335 (this is far from the paraxial case) and this explains the small difference between this prediction and the results shown in figure 3.5.

From the plot shown in figure 3.5, we predict that for A=4.57, the $1/e^2$ confocal intensity beam waist is 1.15 microns at 1064 nm and the confocal PSF full

width at half maximum (FWHM) is 1.38 microns. From this point response, we can generate a line or edge response of the system that we can compare to actual measurements. Figure 3.6 displays the confocal edge response for the CMaRS for A=4.57. The 20-80% rise for this edge is equal to 1.12λ when normalized to the wavelength. At 1064 nm, the predicted edge response is 1.19 microns.

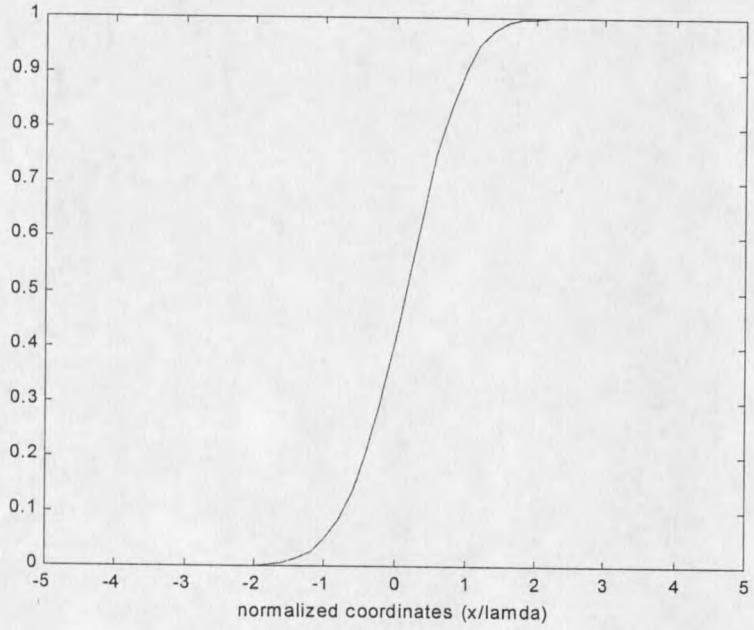

Figure 3.6 Edge response (intensity) for the simplified confocal microscope plotted versus x/λ (where x is a radial dimension in the focal plane). A=4.57, NA= 0.25.

Axial Response

The cross-sectioning abilities of a confocal microscope are dependent upon its depth of focus or axial response, also called V(z). Intuitively, we know that high NA objective lenses will have a tight focus and therefore a narrow axial response.

$$\frac{I(u)}{I(0)} = \frac{A^2}{\quad} \frac{(1 - e^{-2A} - Ae^{-A}\cos u)}{\quad} \qquad (3.5)$$

Equation 3.5 shows the axial response of the ideal FCOM to a perfect plane reflector [25].

where $u=2kz(1-\cos\theta)$ is a dimensionless defocus parameter and θ is the angle corresponding to the numerical aperture of the microscope such that $NA=\sin\theta$. Figure 3.7 is a plot of equation 3.5 for four different values of A. The FWHM at 1064 nm is 14.3 microns.

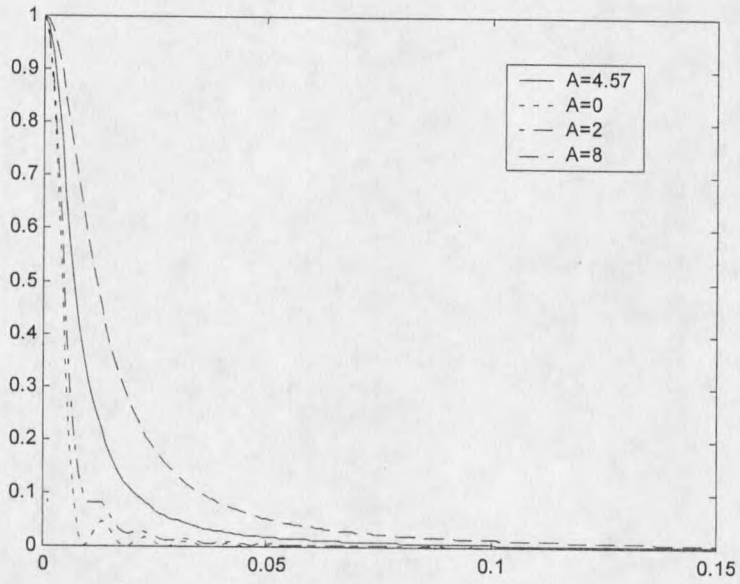

Figure 3.7 Normalized projected axial response of a confocal microscope for different values of A, NA=0.335. The horizontal axis is in units of mm/λ.

Efficiency

It is clear from the theoretical axial response and the PSF that a value for the *A*-parameter smaller than 4.57 is desirable. However, these performance measures are a trade-off with light efficiency. As *A* decreases in size, the beam waist is getting

much larger than the pupil, thus decreasing the amount of light allowed through the system. Figure 3.8 shows the round-trip efficiency for the CMaRS 1064 as the waist of the incoming beam is varied and incident upon a square aperture. This plot assumes that the only losses in the system are due to the limiting size of the aperture. The beam is assumed to be a Gaussian. The zig-zag in the beam path is taken into account, as the 22.5° angle of incidence effectively reduces the size of the scan mirror with respect to an incoming beam. The actual beam waist ($1/e^2$ intensity radius) of 0.5 mm corresponds to an efficiency of 97% round-trip for 1064 nm. This high efficiency was chosen at the expense of spatial resolution and axial response for the Raman spectroscopy portion of the system. Light collection is an important

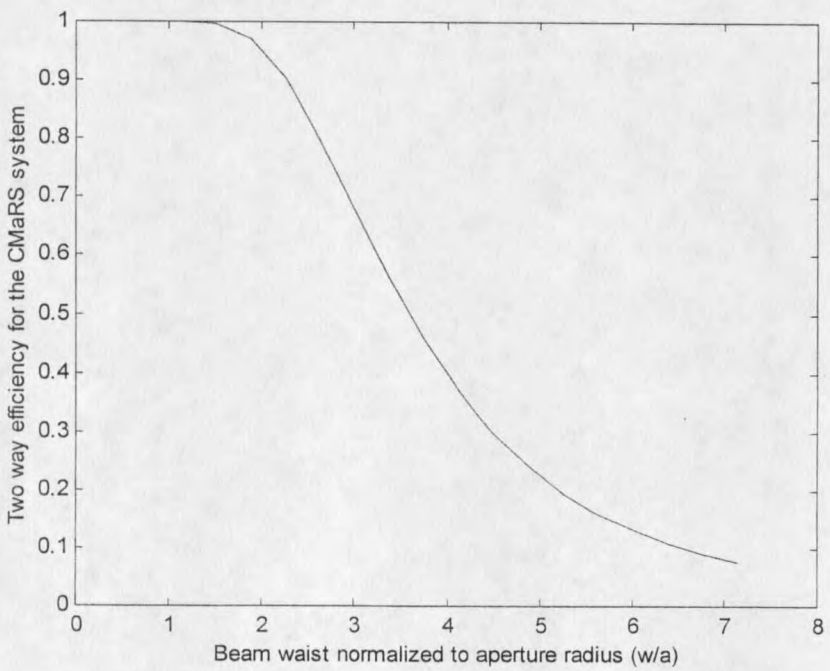

Figure 3.8 Two way efficiency of the confocal microscope.

parameter to enable quality spectra and this governed the value of A that was chosen.

Other factors that influenced this choice were the off-the-shelf optics available, the fixed size of our scan mirror, and the trade-off between the field of view vs. N.A. An *A* parameter equal to 4.57 balances all these considerations well.

Zemax simulation

Zemax is an optical design software program used to simulate the optical performance of the CMaRS. This is particularly valuable in addition to the

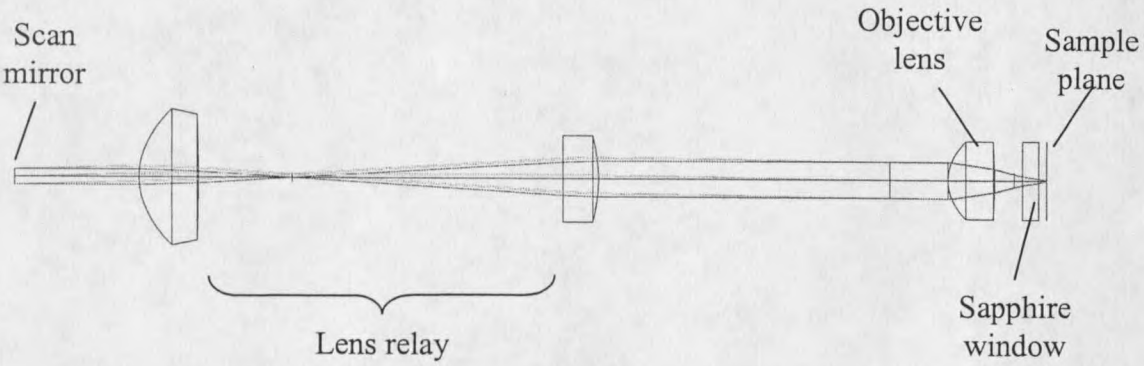

Figure 3.9 Zemax layout for performance optimization and simulation of CMaRS.

MATLAB analysis because it allows us to insert the actual aspheric lenses used by the CMaRS into a simulation. Figure 3.9 shows the layout of the optical system considered and optimized with the scan mirror taken as the aperture stop. Analysis was performed at 852 nm and at 1064 nm, both on-axis and at two different scan angles corresponding to fields of view of 100 microns and 300 microns. The 1064 nm data will be presented since experimental verification of these performance measures will be presented for 1064 nm in Chapter 5.

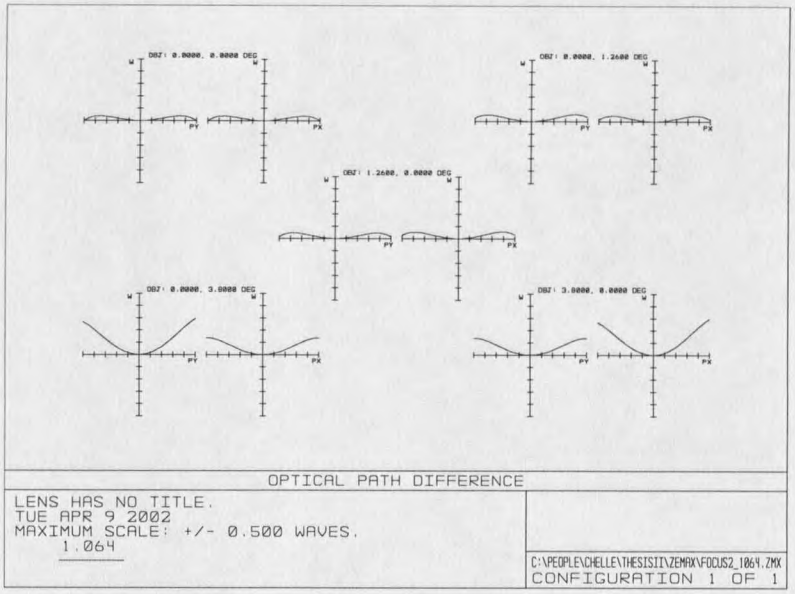

Figure 3.10 Optical path difference plots for on and off-axis beam paths in the 1064 lens system.

Optical Path Difference The optical path difference (OPD) is plotted for the on-axis case as well as for two different scan angles in x and in y (see figure 3.10). These optical scan angles are 1.26 and 3.8 (0 to peak, measured at the mirror) which correspond to a field of view of 100 microns and 300 microns, respectively. The maximum on these axes is 0.5λ, which indicates a reasonable performance of the system. In the case of axial propagation, path differences are within 0.1λ. For the small scan angles (1.26 optical deflection, 0-peak, at the mirror), there is little change from the on-axis case. However, for the larger field of view, especially the axis that is not being scanned begins to exhibit path differences approaching 0.3λ. We can expect to see some change in the image quality at the edge of the field of view for a 300 micron image.

Spherical Aberration The spherical aberration coefficient (as calculated by Zemax) varies from $-(0.1188)\lambda$ to $-(0.1190)\lambda$ as the objective moves through its range of focus. These coefficients are very small and show that there is very little spherical aberration in our image, over the full focus range.

Variable Focus Performance The focus control steps the objective lens forward and reverse along the axis of the beam. At either extreme, the PSF shows no noticeable change. Other issues that could change the PSF are de-centration of the lenses. The lens mounts are subject to human error in fabrication, which ensures that axial alignment will be less than perfect. Zemax simulations showed little difference in performance with a de-center of 0.1 mm (or 4 thousandths of an inch). Mounts for these lenses were given 2 thousandths of an inch tolerance for critical dimensions. This holds the y-axis (vertical) accurately on center, but precision in horizontal alignment is reliant upon assembly.

Opto-mechanical Design

Design Constraints

The CMaRS was conceived as a part of the Mars Instrument Development Program (MIDP). With a surface exploration of Mars as its goal, primary design concerns are size, weight and power. The CMaRS instruments described in this thesis are breadboard instruments, which means they are prototypes in the development towards a flight instrument. The design has attempted to minimize volume, mass, and

power consumption while serving as a proof of concept and leaving room for any minor adjustments and additions.

This prototype does not take into consideration many of the environmental factors a flight instrument must be prepared for. The temperatures a Mars science instrument will be exposed to both in flight and on the surface of Mars (at the middle latitudes) are between -110° C and +40° C. [27] These are not necessarily operating temperatures, but temperatures the instrument must be able to withstand and under which the instrument must maintain its structural and operational integrity. Considering the locations on the surface of Mars where the CMaRS would likely be sent, the operation range for the CMaRS is between -80° C and -10° C. It is possible to use a thermal insulation system and heating element inside the probe to raise the lower end of these specifications to -40° C. The CMaRS 852 and CMaRS 1064 prototypes are designed for operation at room temperature and have yet to undergo thermal modeling and testing for the extreme temperature swings it must withstand for a Mars mission. The optical mounts and the probe exterior have been constructed almost entirely out of aluminum to minimize thermal expansion differences, and adhesives and electrical components have been chosen which can cycle to -50° C, but the instrument has not yet been thermally cycled.

Other environmental concerns which this version of the CMaRS does not address and would need to be considered for a planetary exploration instrument are outgassing, vibrational testing, acoustic testing, and sealing.

For any type of remote appliction, simplicity in design is most efficient for statistical reasons. Since repair operations on Mars are not feasible, it is important to

minimize opportunities for failure. The CMaRS design avoids moving parts when possible, but a purely rigid instrument was not possible by definition of a confocal scanning microscope.

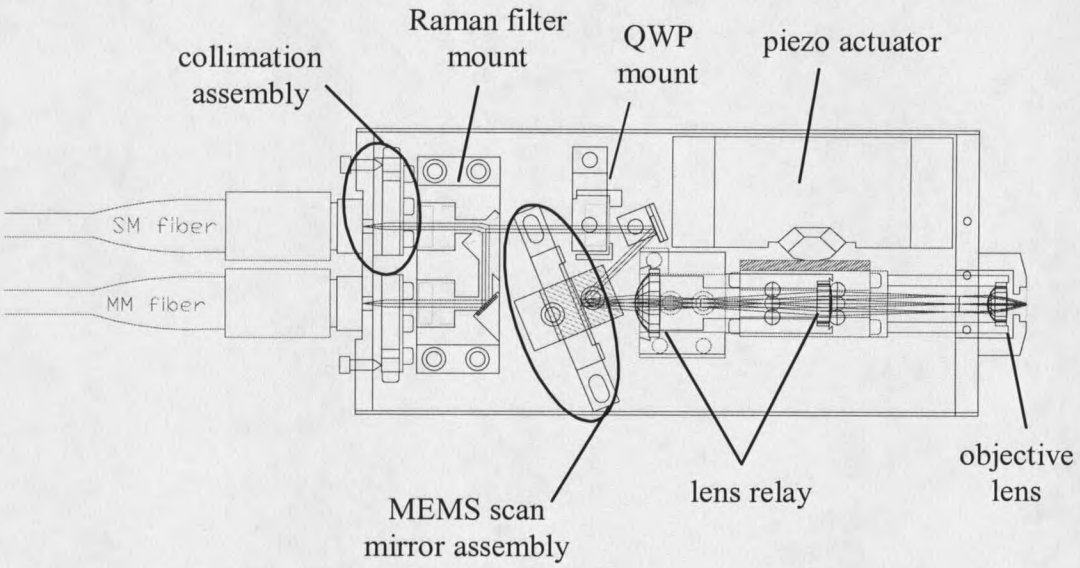

Figure 3.11(a) AutoCAD drawing of probe layout

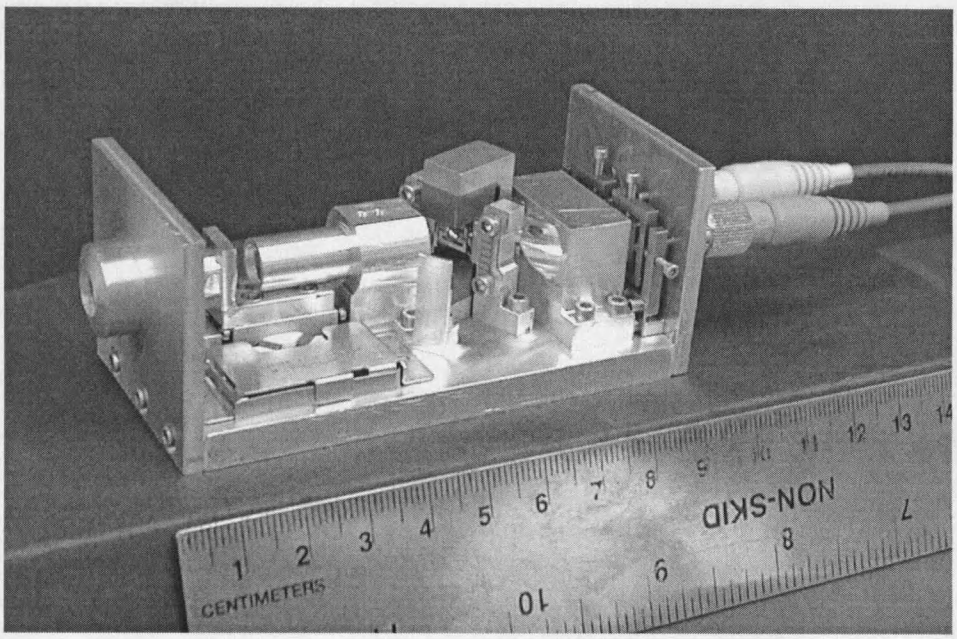

Figure3.11(b) Photograph of CMaRS before any electrical connections were made.

Probe Layout

The probe layout is designed to conserve volume while providing a means of making simple adjustments and alterations to the parts involved. A rectangular base-plate is the foundation, and all pieces are mounted to this base-plate from above or below. Aluminum was chosen as the fabrication material for its ease of acquisition, low density and non-magnetic property. Additionally, aluminum is relatively easy to machine.

Figure 3.11(a) shows an AutoCAD drawing of the probe layout from a top view. It identifies most of the individual parts in the probe and their relative location. This section will discuss in detail the integral mechanical elements in the probe, such as the scan mirror, the collimation unit, and the focus control. Additionally, the mounts for all elements, both optical and mechanical will be described briefly.

Mechanical Elements

MEMS Scan Mirror The MEMS scan mirror, built by Microvision, Inc. is a bi-axial scan mirror fabricated from single crystal silicon via bulk micromachining technology. Figure 3.12 shows the mirror's general architecture. The system consists of two hinged concentric plates, which operate simultaneously and perpendicularly to each other to give the mirror a full range of motion around the x and y axes. The inner plate scans the beam horizontally (as the mirror rotates about the vertical axis) and is driven electrostatically. This axis is driven at resonance (approximately 19 kHz) and thus referred to as the 'fast scan.' The outer plate is rotated via a magnetic

drive, scanning the incident laser beam vertically. This axis is driven off-resonance at 30 Hz, thus referred to as the 'slow scan'.

The bulk silicon layer is epoxied to a ceramic or glass substrate which provides structural support and contacts for electrical connections. Including the substrate, this MEMS device measures 12.8 mm x 7.2 mm x 1 mm thick, though the mirror, itself, measures only 1.4 mm x 1.4 mm. The size of the overall system is most affected by the magnetic drive, which requires relatively large rare earth magnets to generate a constant magnetic field across the mirror [28]. Including the magnets and aluminum mount for the mirror, the scan mirror system measures 1.1" x 1.1" x 0.55 " deep.

The slow scan is driven by an alternating current passing through a magnetic field. The NdBFe24H magnets and their stainless steel return path (manufactured by Magnet Applications, Inc.) envelop the mirror, creating a constant magnetic field of approximately 5 mGauss across the face of the mirror. The outer plate of the machined silicon acts as a substrate for a current coil as shown in figure 3.12. The CMaRS SC module generates a sawtooth waveform which drives an alternating current through the coil and torques the mirror. Driving the slow scan off-resonance not only keeps the part from self-destructing due to enthusiastic scan angles, it puts the mirror in a linear region of its frequency response curve and allows the slow scan to be controlled open-loop.

The electrostatic drive requires a high voltage sinusoidal signal sent alternately to the two electrodes located on the ceramic substrate directly beneath the scan mirror. This scan axis has an extremely high Q factor, due in part to the high resonant frequency at which it is run. Because of this, if the resonant frequency of the

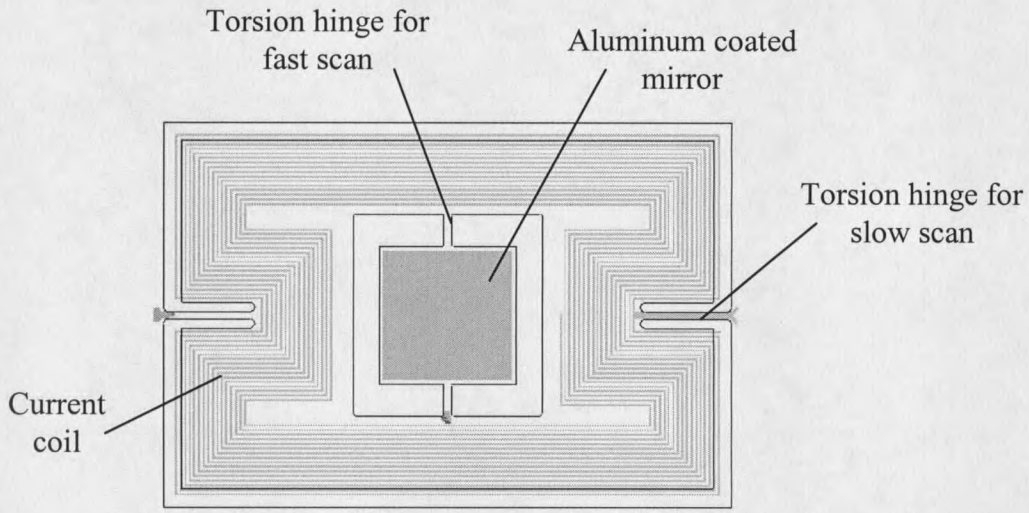

Figure 3.12 AutoCAD drawing of the MEMS scan mirror (courtesy of Microvision). Bonding pads for electrical connections are not shown.

mirror were to change due to environmental factors while the scan is running, the scan angle would loose amplitude very quickly. To avoid drastic changes in scan amplitude, Microvision has incorporated a sensing system and feedback control of the drive frequency [28].

The Microvision MEMS scan mirror meets all of the required specifications for use in the CMaRS instrument. Mechanical scan angle (MSA) measures the amplitude of the angle, 0 to peak, that the mirror moves while scanning. Microvision, Inc. reports achieving a MSA of 6.7° on the fast scan axis and 4.8° on the slow scan axis [28]. This deflection is more than adequate for the CMaRS imaging system.

Images from the CMaRS table-top proof instrument have a field of view of 300 microns, corresponding to a MSA of only 2°. The CMaRS system is therefore not limited by the scan mirror.

Focus Control Control of the depth of focus is achieved using a piezo driver built by Micropulse Systems, Inc. (located in Santa Barbara, CA) to move the objective lens along the z-axis. The L-104 driver (diagram in figure 3.13 and photograph in figure 3.14) is designed to operate in pairs to achieve linear or rotary motion of a separate element. However, the CMaRS probe uses only one L-104 driver to move a conventional linear slide back and forth. The objective lens mount is secured to the top of the linear slide, and mechanical stops ensure a maximum of one millimeter of total motion.

The L-104 driver consists of a spring loaded stainless steel block adhered to

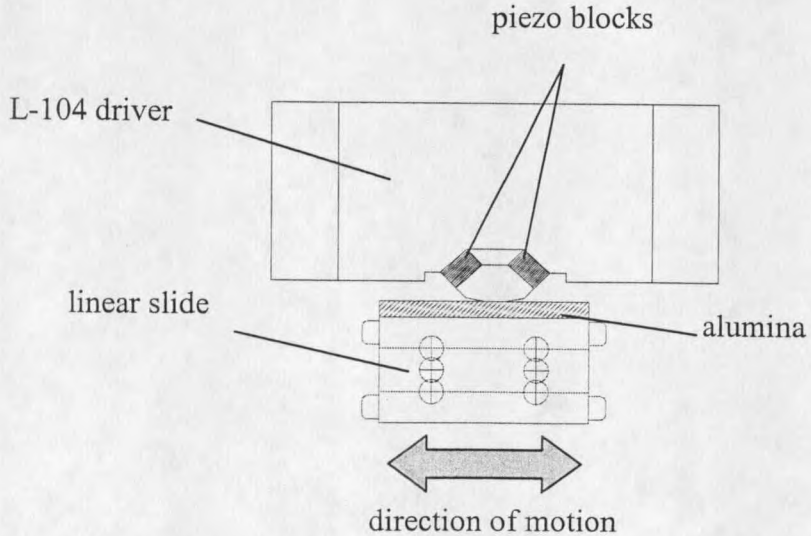

Figure 3.13 Diagram of L-104 piezo driver and linear slide.. The objective lens mount is fastened to the top of the linear slide through the holes shown. The slide and the objective lens then move in the direction of the arrow.

two piezo blocks attached to either side of an alumina wedge. The alumina makes contact with the element that moves, and the piezo blocks are activated individually to make the slide move in one direction or the other. 'Activating' the piezo block consists of sending it a 134 kHz sine wave at approximately 600 volts peak to peak.

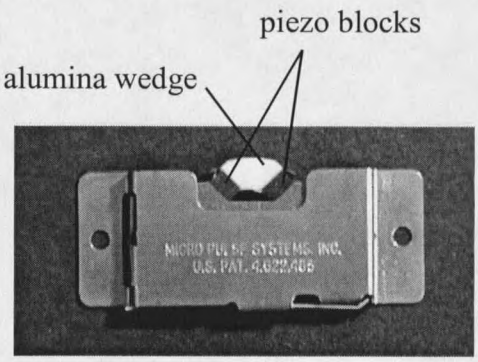

Figure 3.16 Photograph of the L-104 piezo driver.

Pulsing this signal for a known time increment moves the slide a discreet distance. The L-104 driver operates on frictional principles. With each oscillation, the piezoceramic element is stretched and compressed, pushing the alumina wedge against the slide and then pulling it away. In effect, the slide is hammered (in very small increments) in one direction, and then the opposite piezo block is activated, and it is hammered back to its starting point [29]. This constant hammering makes it necessary to choose a material with like hardness to the alumina wedge for the driven face of the slide. The slide is made of aluminum, which is extremely soft when compared to alumina, so a piece of alumina was epoxied to the side of the linear slide.

Micropulse Systems specifies their L-104 driver pair to have a resolution of two micro-inches (0.05 microns) [29]. Since the CMaRS does not use the L-104 driver in its intended fashion (we are using one driver instead of a pair) these

attempt to keep the motion of the lens as linear as possible. One full revolution of the screw moves the lens 0.0125 inches.

Control over z-axis position is achieved similarly. The x-y mount shown in Figure 3.15 is attached to the end-plate of the CMaRS via the three mounting holes and a piece of steel shim and a 'spacer block.' The end-plate is the piece the optical fibers and electrical cable are connected to, and also serves as one of the exterior walls for the probe. A translation screw maintains a set distance between the end-

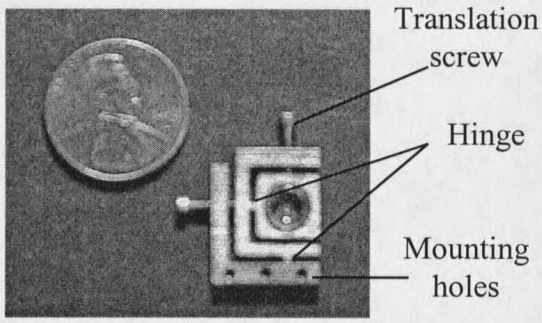

Figure 3.15 Collimation lens mount for x-y positioning of lens.

piece and the collimating lens mount. The shim acts as a hinge and translation of the lens is achieved by turning the screw and pushing the lens away from the end-plate. The shim steel piece is bent to oppose this motion before assembly, and is an effective spring.

This collimation assembly is a functional solution for the application. It is not an answer for a situation desiring frequent adjustments of the collimation or beam position as fatigue in the hinges would quickly become a problem.